First-principles investigation of the structural, electronic and optical properties of olivine-Si_3N_4 and olivine-Ge_3N_4

2006 J. Phys.: Condens. Matter 18 10663

(http://iopscience.iop.org/0953-8984/18/47/012)

INSTITUTE OF PHYSICS PUBLISHING JOURNAL OF PHYSICS: CONDENSED MATTER

J. Phys.: Condens. Matter **18** (2006) 10663–10676 doi:10.1088/0953-8984/18/47/012

First-principles investigation of the structural, electronic and optical properties of olivine-Si_3N_4 and olivine-Ge_3N_4

Hao Wang[1], Ying Chen[1], Yasunori Kaneta[1] and Shuichi Iwata[2]

[1] Department of Quantum Engineering and Systems Sciences, School of Engineering, The University of Tokyo, Hongo 7-3-1 Bunkyo-ku, Tokyo 113-8656, Japan
[2] Graduate School of Frontier Science, The University of Tokyo, Hongo 7-3-1, Bunkyo-ku, Tokyo 113-8656, Japan

E-mail: hao@qs.t.u-tokyo.ac.jp

Received 4 July 2006, in final form 29 September 2006
Published 13 November 2006
Online at stacks.iop.org/JPhysCM/18/10663

Abstract

Si_3N_4 and Ge_3N_4 are important structural ceramics with many applications because of their outstanding high-temperature and oxidation-resistant properties. Two stable phases of them, α and β, have thus far been synthesized. The high-pressure and high-temperature spinel phases of these two materials were noticed to have wide, direct electronic band gaps that are comparable to those of the promising newly developed solid-state optoelectronic materials such as lasers and LEDs. Another high-pressure and high-temperature phase, the olivine phase, has also attracted attention recently. In the present work, the structural and electronic properties of the new olivine nitrides Si_3N_4 and Ge_3N_4 are studied by the FLAPW method with PBE-GGA exchange and correlation potential. The stability of the two materials and the transition pressure are investigated. It is found that olivine-Ge_3N_4 is not stable and is difficult to be observed, while olivine-Si_3N_4 can be synthesized under appropriate conditions. The atomic sites have been optimized and the ground-state properties such as equilibrium lattice constant, bulk modulus, band structure and density of states have been obtained. Furthermore, the dielectric function has been calculated based on the random phase approximation.

(Some figures in this article are in colour only in the electronic version)

1. Introduction

Polymorphs formed from elements in group IV and group V make an interesting and important class of materials. Silicon nitride (Si_3N_4) is a well-known material because of its high fracture toughness, hardness and wear resistance [1, 2]. Another well-researched polymorph is Ge_3N_4.

The existence of several solid phases and the phase transitions among them have been attracting interest for years. Three phases, α ($P31c, hp28$), β ($P6_3/m, hp14$) and γ (spinel, $Fd\bar{3}m$, $cF56$) phases of Si_3N_4 and Ge_3N_4 are well known from experiments [3–7]. Both the α and β phases for Si_3N_4 and Ge_3N_4 are stable under ambient pressure, while the β phase is more stable than α phase. The α phase undergoes a transition into the β phase upon heating; however, the $\beta \rightarrow \alpha$ phase transition has not yet been observed. The high-pressure phases of them are the γ phase. γ-Si_3N_4 was first synthesized under a pressure of 15 GPa and at a high temperature of 2000 K [7]. It exhibits a wide direct band gap of 3.45 eV, though this is much smaller than those of α- and β-Si_3N_4 which have indirect band gaps [7–10]. The $\beta \rightarrow \gamma$ phase transition of Ge_3N_4 occurs near 12–15 GPa and above 1273 K [9]. β-Si_3N_4 undergoes a transition to the γ phase by a fast reconstructive process at a pressure above 20 GPa [11]. The γ phase is an isostructure of cubic-C_3N_4, which is a new superhard substance predicted theoretically by Teter *et al* and whose bulk modulus is even larger than the value of diamond [12]. It has been shown that γ-Si_3N_4 and γ-Ge_3N_4 have wide, direct electronic band gaps that are comparable to those of the promising newly developed solid-state optoelectronic materials such as GaN, InN, AlN [13], which have induced intensive researches on group VIA and VIB elements spinel nitrides from their structural, electronic properties to thermodynamic and mechanical properties [14–17].

A new phase in Ge_3N_4 is a high-pressure phase with olivine-type structure ($Pnma, oC28$) predicted theoretically by Dong *et al*. It was indicated that a transition to a metastable olivine phase in Ge_3N_4 could occur under appropriate pressure and temperature, if the $\beta \rightarrow \gamma$ transition could be bypassed. They suggested that this could be achieved by exploiting the slow kinetics of the reconstructive transformation at low temperature [13]. Since in some isoelectronic oxides, such as Mg_2SiO_4, the olivine structure is the ground-state structure and it transforms into spinel at high pressure, it is interesting to explore further the olivine phase in nitrides. However, detailed information of the crystal structure, the stability and the condition of the phase transition of the olivine phase are not clear yet.

In present paper, we investigate the phase stability, and the structural, electronic and optical properties of both Si_3N_4 and Ge_3N_4 by *ab initio* calculations using the full-potential linearized augmented plane wave (FLAPW) method [18]. Our results show that the phase transition to olivine structure is rather difficult to occur in Ge_3N_4 while it has a possibility of taking place in Si_3N_4.

The crystal structures of Si_3N_4 and Ge_3N_4 are described in section 2, which is followed by the calculation method and parameters in section 3. Results and discussion are given in section 4. Section 5 contains a summary and conclusion.

2. Crystal structure

Both Si_3N_4 and Ge_3N_4 have two stable structures at ambient conditions, α and β. The higher-symmetry β phase ($P6_3/m, hp14$) has a hexagonal lattice, while the lower-symmetry α phase ($P31c$, $hp28$) is trigonal. Both structures consist of a tetrahedral network with each Si or Ge connected by three-coordinated N atoms; these have pyramid-like form in the α phase, whereas the β phase can be regarded as stacking along the c-axis with a two-layer repeat pattern. In the spinel-structured ($Fd\bar{3}m$, $cF56$) polymorph γ-Si_3N_4 and γ-Ge_3N_4, Si or Ge atoms are assumed to be in both tetrahedral and octahedral coordination to nitrogen. The olivine-named mineral is often used to designate members of the solid solution series bound by the end-members forsterite (Mg_2SiO_4) and fayalite (Fe_2SiO_4). The olivine structure type is commonly described as a somewhat distorted hexagonal close-packed array of anions in which one-eighth of the tetrahedral and one-half of the octahedral interstices are occupied by cations. This structure type can be designated as A_2BX_4, where A refers to octahedrally

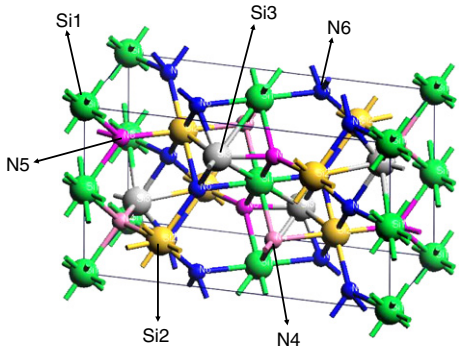

Figure 1. The crystal structure of olivine-Si_3N_4.

Table 1. The Wyckoff parameters for each atomic species [19].

Atom	Wyckoff site	Coordinates
Si1	4a	$(0, 0, 0), (1/2, 0, 1/2)$ $(0, 1/2, 0), (1/2, 1/2, 1/2)$
Si2, Si3 N4, N5	4c	$\pm(u, 1/4, v)$ $\pm(u + 1/2, 1/4, 1/2 - v)$
N6	8d	$\pm(r, s, t), \pm(r, 1/2 - s, t)$, $\pm(r + 1/2, 1/2 - s, 1/2 - t)$, $\pm(r + 1/2, s, 1/2 - t)$

coordinated cations, B refers to tetrahedrally coordinated cations, and X refers to anions which are coordinated by three A cations and one B cation. In a unit cell of olivine-Si_3N_4 or olivine-Ge_3N_4, A-type Si or Ge occupies the centres of distorted nitrogen octahedra, whereas B-type Si or Ge is tetrahedrally coordinated to nitrogen.

The olivine structure has space group $Pnma$, Pearson symbol $oC28$ with 8 A-type Si or Ge, 4 B-type Si or Ge and 16 N atoms which form 6 non-equivalent atom groups, Si1(Ge1), Si2(Ge2), Si3(Ge3), N4, N5 and N6. The Wyckoff sites and internal structural degrees of freedom are given in table 1, where the number following the element symbol of the atom is the identifier of the symmetrically non-equivalent atom group in the unit cell. These internal parameters have not been reported yet and need to be determined first in the calculations. The crystal structure of olivine-Si_3N_4 is shown in figure 1, where Si1 and Si2 correspond to A, and Si3 corresponds to B.

3. Calculation method and calculation parameters

In order to investigate the structural and electronic properties of olivine-Si_3N_4 and Ge_3N_4, we performed calculation based on the local density approximation (LDA) with the generalized gradient approximation (GGA) [20, 21]. The calculations were performed using WIEN2k with a scalar relativistic effect [22]. The PBE-GGA was employed for the exchange and correlation potential [21]. The linearized augmented plane wave (LAPW) and augmented plane wave with local orbitals (APW + lo) methods were adopted as basis because the highest efficiency is found for a mixed basis set. The 'physically important' l quantum numbers are treated by APW+lo but the higher values of l were treated by the LAPW method [23]. Also for the

low-lying valence states, semi-core states, the local orbital (LO) was utilized. The basis set of Si, Ge and N for valence states used in the present calculations was

Si: $(2p^6)3s^23p^2$,
Ge: $(3d^{10})4s^24p^2$,
N: $(2s^2)2p^3$;

here, the $(2p^6)$ orbitals of Si, $(3d^{10})$ orbitals of Ge and $(2s^2)$ orbitals of N are treated as semi-core states. For the potential and charge density representation, the maximum l-value for partial waves used inside atomic spheres was 10 and the one used in the computation of non-muffin-tin matrix elements was 4. In the interstitial region the basis functions were represented by Fourier series and the plane wave cut-offs of calculations were all set to be above 25 Ryd. The muffin-tin radii for Si, Ge and N were used (1.6, 1.7 and 1.5 au, respectively). The tetrahedron method was used for efficient sampling of the first Brillouin zone (BZ), and 126 points in the irreducible BZ [25], which corresponds to 1000 k-points in the whole BZ, were found to give a good convergence of the total energy and the ionic forces.

In order to obtain the internal structural parameters for Si_3N_4 and Ge_3N_4, a reverse-communication trust-region quasi-Newton method from the Port library [26] was applied to optimize the equilibrium position of all individual atoms. Further optimization was performed with the constraint of maintaining the corresponding space-group symmetry.

4. Results and discussions

The main objective of present research was to investigate the unknown properties of newly predicted olivine-Si_3N_4 and olivine-Ge_3N_4. However, in order to provide a consistent comparison of olivine phase with other phases which have already been reported, as well as a confirmation of accuracy of the present work, all calculations were been carried out for α, β and γ phases of both Si_3N_4 and Ge_3N_4 within the same theoretical framework. We present all results for the γ phase together with the olivine phase, but only include the β phase results in the discussion of phase stability and energy gaps.

4.1. Structural optimization and stability

So far olivine-Si_3N_4 and olivine-Ge_3N_4 have not been researched sufficiently and no structural parameters have been published. It was necessary to optimize the lattice parameters first. There are several steps for determining the equilibrium lattice parameters. First the ideal atomic positions of olivine phase material shown in table 2 were used with the lattice parameters from figure 3 in the paper by Dong *et al* [13]. Then the atomic positions were relaxed globally using the force-minimization technique. Afterwards, the total energies were calculated by fixing both the optimized atomic positions and c/a ratio with different compressed and expanded volumes. Finally, by fitting the total energies versus volume to Murnaghan's equation of state [28], we derived the equilibrium properties such as lattice parameter, the bulk modulus B, and the pressure derivative of the bulk modulus B' from the equation of state.

The calculated internal coordinates for olivine-phase and spinel-phase Si_3N_4 and Ge_3N_4 are listed in table 2. It can been seen that for the γ phase, our results are very close to the measurements and other calculations, which confirms the reliability of our approach. For the olivine phase, the results show a small deviation of the optimized structures from the ideal ones. These calculations provide detailed information on the internal parameters for both olivine-Si_3N_4 and olivine-Ge_3N_4 for the first time.

Table 2. Optimized internal parameters in γ-, olivine-Si_3N_4 and γ-, olivine-Ge_3N_4 in unit cell.

		Olivine phase					γ phase
	Atom	u	v	r	s	t	w
Ideal							
	Si2 or Ge2	0.25	0				0.3750
	Si3 or Ge3	0.0833	0.375				
	N4	0.0833	0.75				
	N5	0.4167	0.25				
	N6			0.1667	0	0.2500	
Optimized							
Si_3N_4	Si2	0.2900	0.9662				0.3838
	Si3	0.0918	0.4398				
	N4	0.0951	0.8127				
	N5	0.4376	0.2505				
	N6			0.1527	0.0011	0.2736	
Experiment							0.3875[a]
							0.3833[b]
Other calculations							0.3843[c]
							0.3844[d]
Ge_3N_4	Ge2	0.2800	0.9887				0.3833
	Ge3	0.0945	0.4476				
	N4	0.0940	0.8210				
	N5	0.4372	0.2448				
	N6			0.1611	0.0052	0.2620	
Experiment							0.3827[e]
Other calculations							0.3830[f]
							0.3841[d]

[a] Reference [4]; [b] Reference [24]; [c] Reference [10]; [d] Reference [27]; [e] Reference [5]; [f] Reference [13].

The results of calculated equilibrium properties of the four systems are summarized in table 3, together with available experimental data and other calculations. For the equilibrium lattice constants, one sees that our results for the γ phase (14.7526 au for Si_3N_4, 15.7137 au for Ge_3N_4) achieve an excellent agreement with the experiments (14.7399 au for Si_3N_4, 15.6847 au for Ge_3N_4) [4, 6], better than all other calculations. Within same theoretical framework, the present calculation obtained the equilibrium lattice constants of olivine phase as $a = 18.7717$, $b = 10.5769$, $c = 8.6712$ au for Si_3N_4, and $a = 19.7117$, $b = 11.1474$, $c = 9.1019$ au for Ge_3N_4, respectively.

Shown in figure 2 are total energy versus volume curves for the β, γ and olivine phases of Si_3N_4 and Ge_3N_4. The solid line represents the β phase, the dashed line the γ phase, and the dotted line the olivine phase. For both Si_3N_4 and Ge_3N_4, the results show that the β phase is most stable at the ground state; it is possible to transform it into the γ phase under a high pressure, which coincides with the experimental observations. Another high-pressure phase, olivine, lies higher in energy than the β and γ phases. It is known that in isoelectronic oxides, such as Mg_2SiO_4, the olivine structure is the ground-state structure and it transforms into spinel at high pressure; this is obviously different in the case of nitrides.

In figure 2(a), Si_3N_4, according to our calculation the energy difference between β-Si_3N_4 and γ-Si_3N_4 is 146 meV/atom. By drawing the common tangent line of total energy versus

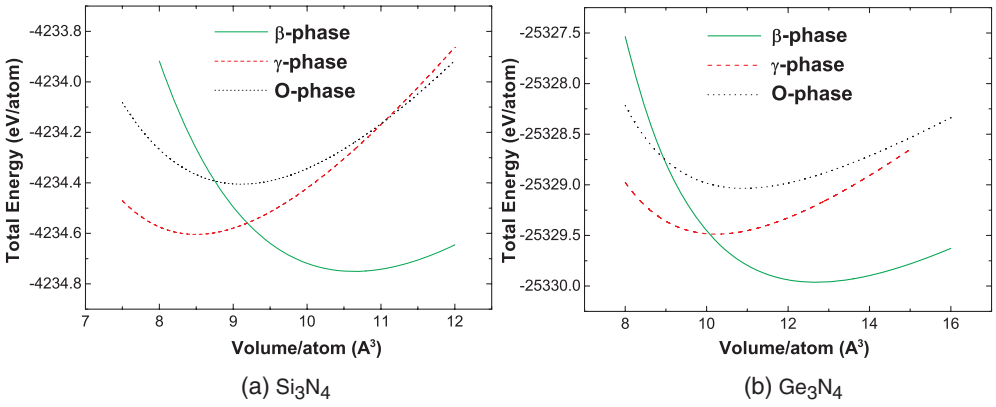

Figure 2. The calculated total energy versus volume curves of (a) Si_3N_4 and (b) Ge_3N_4. The solid line represents the β phase, the dashed line the γ phase, and the dotted line the olivine phase. The parameters are provided in table 3.

Table 3. Equilibrium lattice parameters, band gap and bulk modulus.

	Olivine-Si_3N_4	γ-Si_3N_4	β-Si_3N_4	Olivine-Ge_3N_4	γ-Ge_3N_4	β-Ge_3N_4
Lattice constant						
a (au)	18.7717	14.7526		19.7117	15.7137	
b (au)	10.5769			11.1474		
c (au)	8.6712			9.1019		
Experiment		14.7399[a]			15.6847[b]	
		14.6340[d]			15.5209[c]	
		14.6149[e]				
Others' calculation		14.8102[g]			15.5165[g]	
		14.8092[h]			15.4345[i]	
Band gap (eV)						
	2.99	3.21	4.29	1.55	1.90	2.17
Experiment			4.6–5.3[j]			∼4.5[k]
Other calculations		3.45[g]	4.26[i]		2.22[g]	2.45[i]
		3.45[h]			2.17[i]	
B (GPa)						
	262.9	292.3		182.3	216.3	
Experiment		317 ± 11[f]			296[c]	
Other calculations		280.1[g]			268.6[g]	
		280[h]			240[i]	
B′						
	3.93	4.35		4.61	4.61	
Experiment		2.3 ± 2.1[f]			4.0[c]	
Other calculations		3.76[g]			3.14[g]	
		3.48[h]			4.5[i]	

[a] Reference [4]; [b] Reference [6]; [c] Reference [5]; [d] Reference [21]; [e] Reference [24]; [f] Reference [25]; [g] Reference [27]; [h] Reference [10]; [i] Reference [13]; [j] Reference [30]; [k] Reference [31].

volume curves of β and γ phases which indicates the equilibria of these two phase, the β–γ transition pressure can be estimated from the slope as 7.1 GPa. This implies that the transition from β to γ phase could be easily observed. Looking at olivine-Si_3N_4, we find that it is also

possible to draw a common tangent line of the two energy curves of olivine- and β-Si_3N_4; the transition pressure estimated from the slope is 24.8 GPa. This predicts that when Si_3N_4 is compressed under high pressure from the equilibrium state of the β phase, the phase transition from β-Si_3N_4 to olivine-Si_3N_4 can occur at this pressure if the $\beta \rightarrow \gamma$ transition could be bypassed, and that olivine-Si_3N_4 might exist as a metastable phase. Noticing there is a rather large energy difference of 345 meV/atom between olivine-Si_3N_4 and β-Si_3N_4, such a phase transition into a high-energy state at high pressure generally requires a large amount of internal energy to overcome the energy barrier [13]; the high temperature would be necessary to exert an additional contribution to internal energy from the entropy contribution. In fact, the discussion of such a kind of transformation with a temperature effect should consider the free energy instead of the internal energy at the ground state. However, the internal energy still gives important information about the stability, as shown in current systems.

In figure 2(b), Ge_3N_4, an energy difference of 55 meV/atom is obtained between β-Ge_3N_4 and γ-Ge_3N_4, which agrees with the result obtained by Dong *et al* [13]. The calculated transition pressure between the phases is about 13.7 GPa, which is also in a good agreement with the experiment [9]. However, it is noticed that the bottom point of the energy of olivine-Ge_3N_4 is fully enclosed inside both β- and γ-Ge_3N_4, so that it is impossible to have a common tangent line between either β- and olivine-Ge_3N_4 curves or γ- and olivine-Ge_3N_4 curves, which indicates that olivine-Ge_3N_4 could be difficult to be observed in experiment. In [13], the bottom point of the olivine-Ge_3N_4 curve is out of the β-Ge_3N_4 curve, suggesting the possibility of olivine-Ge_3N_4 being detected. The different results arise from the numerical deviation in the total energy calculations, which we believe to be caused by the methodological accuracy. Generally the FLAPW method we employed in this work is taken as a higher accuracy approach in total-energy values due to its all-electron full potential treatment, whereas with respect to this specific system, to clarify the difference definitely needs further calculation by using the pseudopotential method which Dong applied with same internal parameters as ours to see if our FLAPW result could be reproduced; this will be left for the further calculations and studies.

The calculated bulk moduli B at the equilibrium state are listed in table 3. For γ-Si_3N_4, our result of 292.3 GPa is closer to the experiment value 317 GPa with underestimation by 8% than other calculations, while for γ-Ge_3N_4, 216.3 GPa underestimates the experimental value by 27%, which is a large deviation than expected, but it is closer to Dong's theoretical value [13]. Our results for olivine phases reveal that olivine-Si_3N_4, with 262.9 GPa bulk modulus, is a very hard substance, and also show that for both Si_3N_4 and Ge_3N_4, the spinel phase is a bit stiffer than the olivine phase, which is expected from a slight densification from γ phase to olivine.

4.2. Electronic band structure

The calculated band structures of olivine are shown in figure 3, (a) olivine-Si_3N_4 and (b) olivine-Ge_3N_4, along with the results of (c) γ-Si_3N_4 and (d) γ-Ge_3N_4 for completeness. The top of valence band is set to the zero point of the energy in these graphs. The calculated band gaps for the four systems are listed in table 3; the results for the β phases are also included for comparison.

For these four substances, the band structures appear typically to be semiconductor bands with a direct band gap at the Γ point. The band gap values of olivine-Si_3N_4 and olivine-Ge_3N_4 are 2.99 and 1.55 eV, and those of γ-Si_3N_4 and γ-Ge_3N_4 are 3.21 and 1.90 eV respectively. Both Si_3N_4 phases have wider band gaps than both phases of Ge_3N_4, and the band gaps of γ phases are wider than the ones of olivine phases respectively. Comparing with other reports for spinels, the trends are the same, but our calculations underestimate

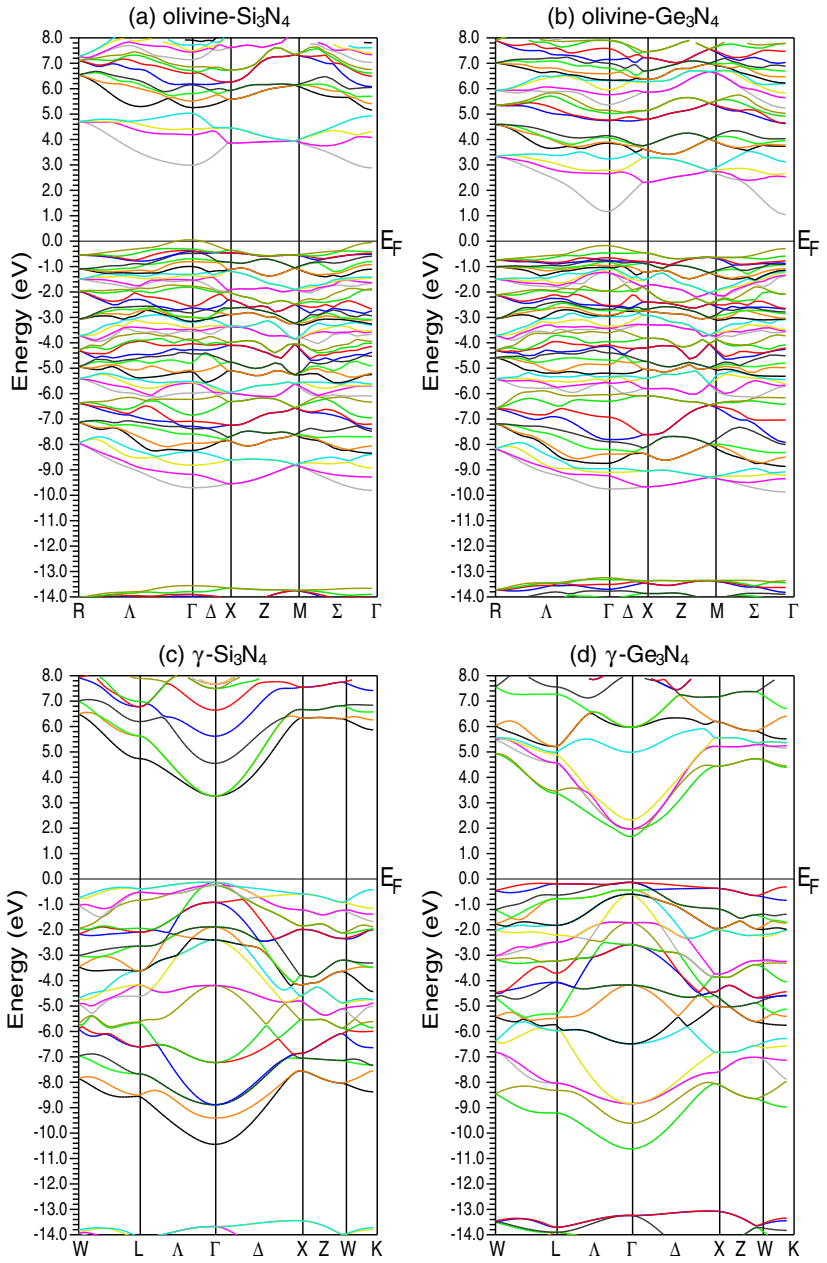

Figure 3. Band structures of the four materials: (a) olivine-Si_3N_4, (b) olivine-Ge_3N_4, (c) γ-Si_3N_4, (d) γ-Ge_3N_4.

the energy gap by 7% to 14%. Noticing that the present calculation employs FLAPW, while other calculations adopted orthogonalized linear combination of atomic orbitals (OLCAO) or ultrasoft pseudopotentials, we expect that these differences in values of gap might be owing to the different theoretical treatments of the exchange–correlation potential and basis function set used in expanding the wavefunctions. Since it is well known that LDA (or GGA) calculations

generally underestimate the band gap of semiconductors and insulators, the real band gaps of them must be wider, which suggests that similar to γ-Si_3N_4, olivine-Si_3N_4 is also a potential wide gap semiconductor material.

In fact, the error originates not only from the LDA (or GGA) but also from the DFT itself due to the discontinuity of the exchange–correlation potential. To make it possible to estimate the degree of the calculated error of energy-band gap, we need to compare our results to the experimental ones. However, to our knowledge, the energy gaps of γ-Si_3N_4 and γ-Ge_3N_4 have not yet been determined experimentally; let us consider the values of β-phase of Si_3N_4 and Ge_3N_4. As listed additionally in table 3, the calculated energy gaps of β-Si_3N_4 and β-Ge_3N_4 are 4.29 eV (indirect), 2.17 eV (direct), while the experimental values are 4.6–5.3, 4.5 eV, respectively. It can be seen that for Si_3N_4 the error is moderate, about 0.31–1.01 eV, whereas for Ge_3N_4, the approximate 2 eV band gap error is about twice that found for Si_3N_4, which is the same trend as Dong's [13]. Nevertheless, we also think that tendency showed in the calculated gaps for different phases is informative for further experiments.

The band structures of olivine-Si_3N_4 and olivine-Ge_3N_4 look similar; so do the cases of γ phase, since Si and Ge are isoelectronic. The upper and lower valence band widths are nearly identical. According to our analysis, the top of valence bands in both olivine-Si_3N_4 and olivine-Ge_3N_4 are dominated mainly by p orbital of N5 and N6. The major difference is in the value of band gap and the states near the conduction band minimum. In olivine-Si_3N_4 the state at Γ point is dominated mostly by the s and p orbitals of Si2 and the p orbital of N6, while in olivine-Ge_3N_4, it is prevailed by the s orbital of Ge2 and Ge1, and the p orbital of N6, N5 and N4. Although an exact discussion of transitions from valence band to conduction band requires calculations of the electronic structures in excited states, as an approximation, the current static electronic band still provides very important information. So it can be approximately identified that the interband transition in olivine-Si_3N_4 will be from N5 and N6 to Si2 and in olivine-Ge_3N_4 it will be from N5 and N6 to Ge2, N4 and Ge1, which will lead to the different behaviour in optical properties of the systems. It is also be noticed that within these four crystals, only the minimum of conduction band in γ-Si_3N_4 is a three-fold degenerate one.

4.3. Density of states

The total electronic density of states (DOS), interstitial electronic density of states and site-decomposed partial density of states (PDOS) of olivine-Si_3N_4 and olivine-Ge_3N_4 are shown in figure 4 (for three kinds of N atom; since their PDOSs are very similar, only N6 is presented). Like the band structures in figure 3, the DOSs of olivine-Si_3N_4 and olivine-Ge_3N_4 also look similar on the gross scale. On close inspection, subtle differences can be seen.

In both cases, the total DOSs have a sharp edge near the top of the valence band, which implies that a lot of electrons are distributed there. The valence band is separated into two parts in both: the lower-energy part is dominated by the s orbital of N atoms, the upper part is formed mainly by the p orbital of N atoms with mixing of a portion of s and p orbitals of the Si(Ge) atom; the interaction between these orbitals provides the strong covalent Si(Ge)–N bonding of the system. For the conduction band, a subtle difference in the peaks above the Fermi level between Si_3N_4 and Ge_3N_4 can be observed, which can be attributed to the different contributions of atoms in octahedral sites in Si_3N_4 and Ge_3N_4. Observing the PDOS of each atom in both systems, one can see the different electronic contributions for octahedral site atoms (Si1 or Ge1, Si2 or Ge2) and tetrahedral ones (Si3 or Ge3) due to the different local environments.

In olivine-Si_3N_4, from the bottom of the conduction band to about 5 eV, s and p orbitals of octahedrally coordinated Si2 prevail mainly, incorporating the p orbitals of N atoms. At about

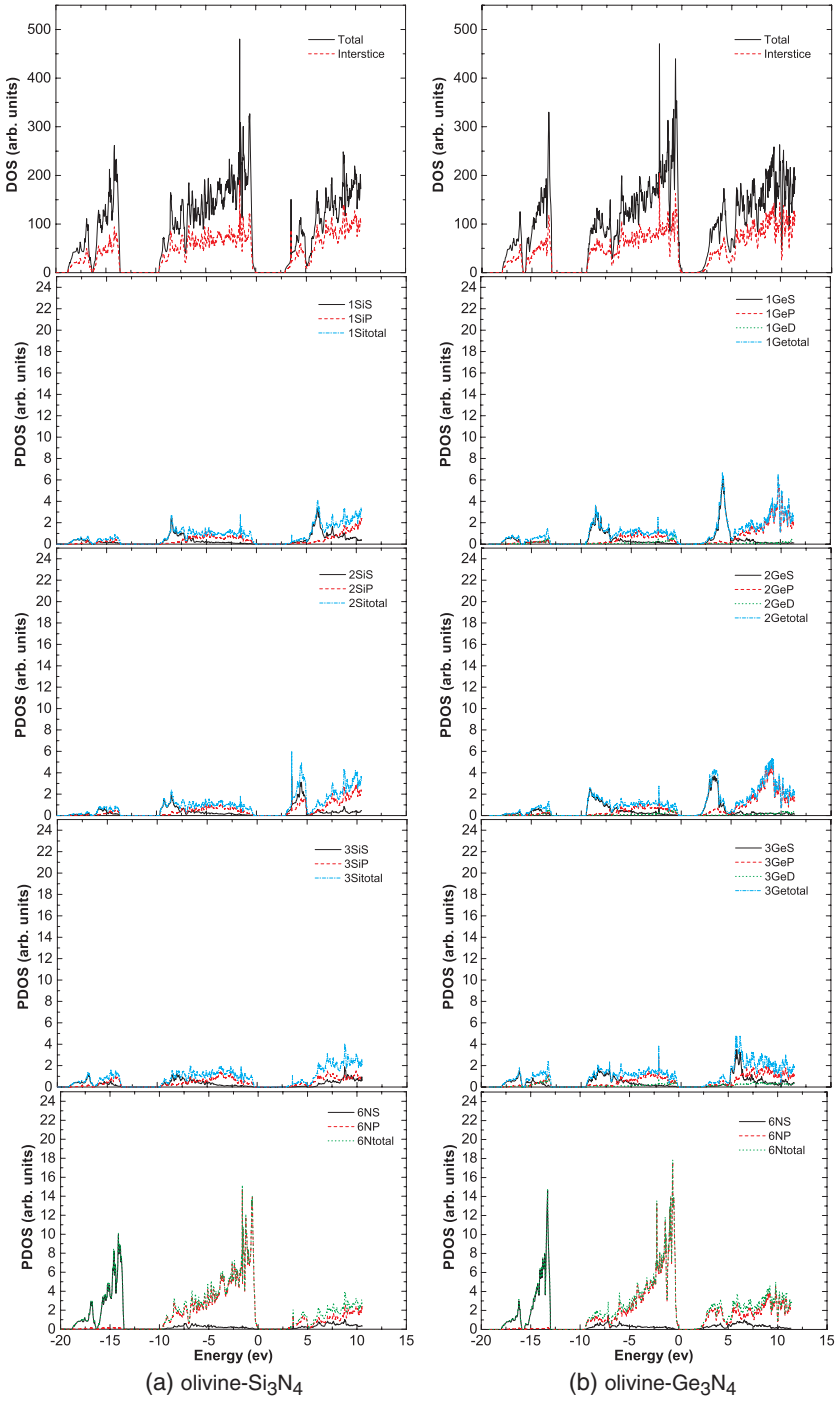

Figure 4. The total electronic density of states and site-projected partial electronic density of states of (a) olivine-Si_3N_4 and (b) olivine-Ge_3N_4 at the Si1(Ge1), Si2(Ge2), Si3(Ge3), and N6 site. Fermi energy is at zero point.

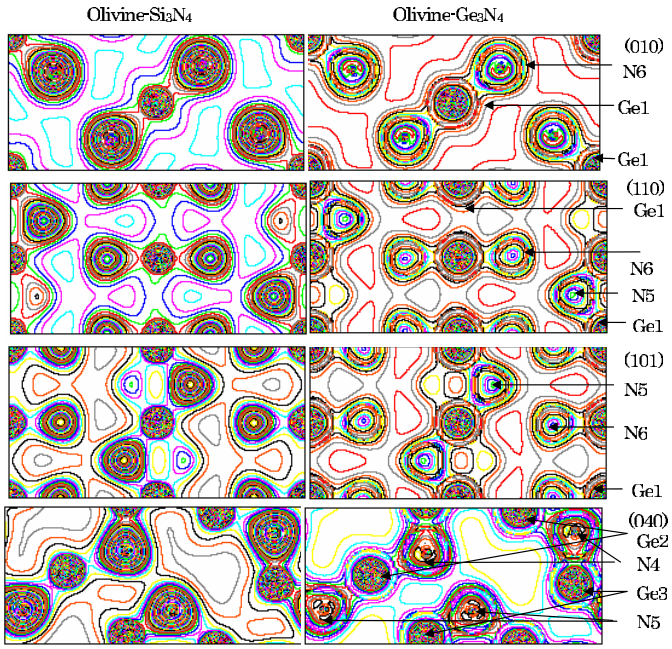

Figure 5. Comparison of the charge distribution on (010), (110), (101), (040) planes of olivine-Si_3N_4 and olivine-Ge_3N_4.

3.6 eV, there is a peak mainly from s and p orbitals of the Si2 atom. It is noticeable that there exists about a quarter of the total valence electrons in the interstitial region which does not belong to muffin-tin sphere of any atom. This is because the olivine phase structure is not close packed and the interstitial space is rather large. Calculation results show that the electrons in the interstitial space are contributed mostly by the valence electrons of Si atoms.

Olivine-Ge_3N_4 has a similar situation in valence band as in Si_3N_4. However, some different features are observed in Ge_3N_4 at the bottom of the conduction band. From the bottom of the conduction band to about 2.5 eV, the s orbitals of octahedral Ge2 and tetrahedral Ge3 occupy states together, with interaction with p orbitals of N atoms; this is different feature from the case in Si_3N_4, so that in the process of interband transition, electrons will move mainly from the p orbital of the N atom to the octahedrally coordinated Si atom in Si_3N_4, but to both octahedral and tetrahedral Ge atoms in Ge_3N_4, which induces some differences in optical properties.

4.4. Charge-density distributions

The valence charge densities of olivine-Si_3N_4 and olivine-Ge_3N_4 are shown in figure 5 where four typical planes ((010), (110), (101), (040)) are displayed together.

The different environment of N atoms in γ and olivine structures under pressure is noticed from the bond lengths in table 4. In the γ spinel phase, the N atom is perfectly tetrahedral or octahedral with strong covalent bonding to Si or Ge, whereas in the olivine structure, the atomic volume decreases slightly from that of the spinel phase: the distances of Si or Ge in a tetrahedral site to the N atom are shortened, but those of Si or Ge in an octahedral site to the N atom vary from shorter to longer than the uniform value in spinel. This implies that some ionic bonding character is introduced in the olivine phase. Considering the fact that the olivine

Table 4. Bond lengths in the four materials.

	Olivine-Si_3N_4	γ-Si_3N_4	Olivine-Ge_3N_4	γ-Ge_3N_4
Bond length (au)				
Octahedral site				
Si1 or Ge1	3.5448(2 × N4)	3.6223	3.7224(2 × N4)	3.8022
	3.5763(2 × N5)		3.8332(2 × N5)	
	3.6849(2 × N6)		3.9721(2 × N6)	
Si2 or Ge2	3.8564(N4)		3.9713(N4)	
	3.6713(N5)		3.8779(N5)	
	3.2834(2 × N6)		3.7011(2 × N6)	
	4.5035(2 × N6)		4.3731(2 × N6)	
Tetrahedral site				
Si3 or Ge3	3.2029(N4)	3.4771	3.3988(N4)	3.6286
	3.2989(N5)		3.5608(N5)	
	3.1802(2 × N6)		3.4674(2 × N6)	

phases have a smaller value of bulk modulus than spinel phases in both Si_3N_4 and Ge_3N_4, based on our results, this leads to a picture that interaction between the octahedral Si or Ge and N takes more important role in bonding than those of tetrahedral sites.

From figure 5, one can see that in the olivine structure, N is larger than the cations, which is due to a rather large portion of valence electrons of Si or Ge atoms being scattering in the interstitial space. The valence charge distribution of N atoms is non-spherical, which reflects the influences of the asymmetrical surrounding atomic configuration, and some covalent bonding character among them. The Ge atom looks to be a much larger ion than Si since the semi-core-like Ge 3d electrons are not strictly confined to the region near the nucleus. It is also noticed that there is a denser charge distribution between N and Si, indicating a stronger bonding, which might explain the reason why olivine-Si_3N_4 has a higher bulk modulus than olivine-Ge_3N_4.

4.5. Optical property

Based on the random phase approximation (RPA) [29], an approximation by many-body perturbation theory to the response of the electron system to a time-dependent electromagnetic perturbation caused by the incoming light, the optical property can be calculated by the real and imaginary parts of the dielectric function ε. The imaginary dielectric function $\varepsilon_2(\omega)$ can be expressed as

$$\varepsilon_2(\omega) = \frac{4\pi^2 e^2 \hbar}{3m^2\omega^2} \sum_{ij} \frac{2}{(2\pi)^3} \int_{\mathrm{BZ}} |M_{\mathrm{ij}}(k)|^2 \delta[\omega_{\mathrm{ij}}(k) - \omega]\, \mathrm{d}^3k \tag{1}$$

where ω is the frequency of incoming light, M_{ij} is momentum matrix element, and m is electron mass. The real dielectric function $\varepsilon_1(\omega)$ is obtained from $\varepsilon_2(\omega)$ by the Kramer–Kröning conversion,

$$\varepsilon_1(\omega) = 1 + \frac{2}{\pi} \wp \int_0^\infty \frac{\omega' \varepsilon_2(\omega')}{\omega'^2 - \omega^2}\, \mathrm{d}\omega' \tag{2}$$

where $\wp$ is the principle value

$$\wp \int_0^\infty \equiv \lim_{\Delta \to 0} \left(\int_0^{\omega - \Delta} + \int_{\omega + \Delta}^\infty \right). \tag{3}$$

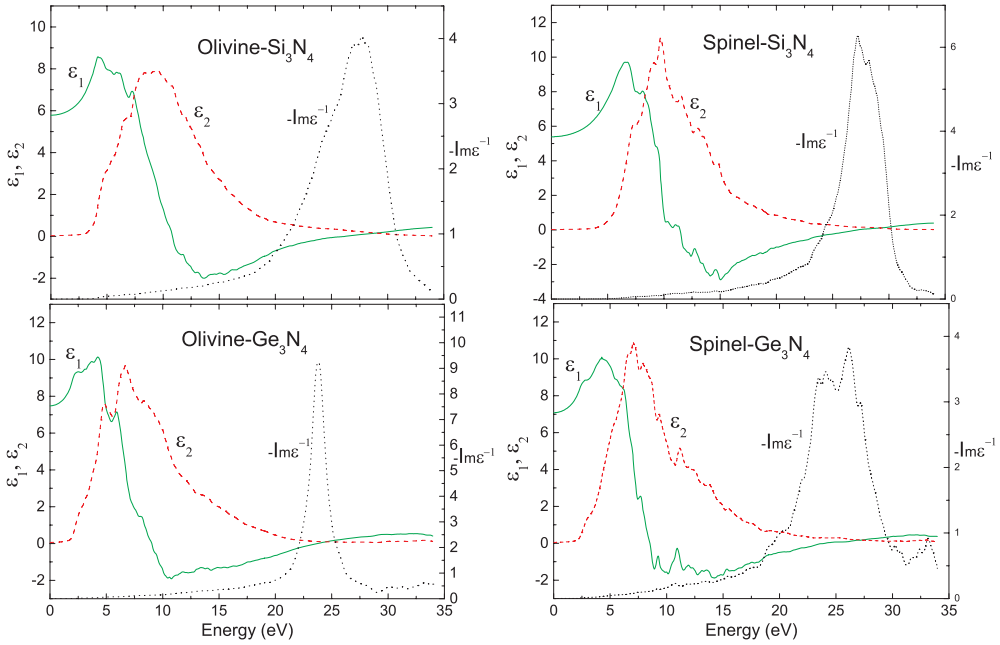

Figure 6. Dielectric function $\varepsilon_1(\omega)$, $\varepsilon_2(\omega)$ and energy loss function of γ-, olivine-Si_3N_4 and Ge_3N_4.

Employing the wavefunction of 126 k-points in the irreducible BZ from the preceding calculation, the frequency-dependent real and imaginary parts of the dielectric function for photon energies up to 30 eV are estimated. The energy loss function can also be evaluated from the dielectric function. The results for the olivine and spinel phases of Si_3N_4 and Ge_3N_4 are shown in figure 6. The solid, dashed and dotted lines represent $\varepsilon_1(\omega)$, $\varepsilon_2(\omega)$ and the energy loss function, respectively. Because of the anisotropy of the olivine structure, the average of three directions of dielectric function is calculated.

The imaginary dielectric function $\varepsilon_2(\omega)$ shown in equation (1) represents the optical absorption in these materials. The spectrum of olivine-Si_3N_4 has a plane absorption peak while olivine-Ge_3N_4 has a sharp one. The absorption peak values of olivine-phase Si_3N_4 and Ge_3N_4 and spinel-phase Si_3N_4 and Ge_3N_4 are 7.96, 9.68, 11.1 and 10.9; they are located at photon energies of 9.51, 6.71, 9.73 and 7.03 eV respectively. It is known that the high peak of $\varepsilon_2(\omega)$ provides fine optical absorption. We noticed that the peaks of $\varepsilon_2(\omega)$ in these four systems are not as high as those of some well know semiconductors, such as Si and GaAs. Further analysis of the details on the electron interband transformation will provide hints in improving the optical absorption property of the materials.

The static dielectric constant, which is $\varepsilon_1(0)$ (excluding any contribution from lattice vibrations), is 5.78, 7.48, 5.39 and 7.08 respectively. $\varepsilon_1(0)$ of both forms of Ge_3N_4 are larger than those of Si_3N_4.

The energy loss functions are also provided in figure 6. The main peak in the energy loss function is defined as the plasma frequency ω_p, the frequency of collective oscillation of the valence electrons in the crystal. Those peaks can be identified from the plot:, 27.7, 23.8, 27.2 and 26.1 eV, for olivine-phase Si_3N_4 and Ge_3N_4 and spinel-phase Si_3N_4 and Ge_3N_4, respectively.

5. Conclusions

A comparative structural and electronic study of a new class of materials, olivine-Si_3N_4 and olivine-Ge_3N_4 has been achieved by a first principles approach. The structure optimization provides the detailed information on internal structure parameters for these two olivine crystals. The stability, electronic band structure, equilibrium structural properties, as well the optical property, are evaluated through this work. Our calculation indicates that olivine-Si_3N_4 might be observed under high pressure and temperature, whereas olivine-Ge_3N_4 would be difficult to be detected. It is found that there is a favourable direct band gap of 2.99 eV and a large bulk modulus of 262.9 GPa for olivine-Si_3N_4; its density of electrons at the top of the valence band is also rather large, which shows the possibility of a high peak of $\varepsilon_2(\omega)$. The calculation suggests that olivine-Si_3N_4 can be a semiconductor with interesting properties and potential technological application.

References

[1] Katz R N 1980 *Science* **208** 841
[2] Belyi V I *et al* 1988 *Silicon Nitride in Electronics, Material Science Monographs* vol 34 (New York: Elsevier)
[3] Kohastu I and McCauley J W 1974 *Mater. Res. Bull.* **9** 917
[4] Priest H F, Burns F C, Priest G L and Skaar E C 1973 *J. Am. Ceram. Soc.* **56** 395
[5] Borgen O and Seip H M 1961 *Acta Chem. Scand.* **15** 1789
[6] Wild S, Grieveson P and Jack K H 1972 *Spec. Ceram.* **5** 385
[7] Zerr A, Miehe G, Serghiou G, Schwartz M, Kroke E, Riedel R, Fuess H, Kroll P and Boehler R 1999 *Nature* **400** 340
[8] Leinenweber K, Keeffe M O′, Somayazulu M, Hubert H, McMillan P F and Wolf G H 1999 *Chem. Eur. J.* **5** 3076
[9] Serghiou G, Miehe G, Tschauner A, Zerr A and Boehler R 1999 *J. Chem. Phys.* **111** 4659
[10] Mo S-D, Ouyang L, Ching W Y, Tanaka I, Koyama Y and Riedel R 1999 *Phys. Rev. Lett.* **83** 5046
[11] Sekine T, He H, Kobayashi T, Zhang M and Xu F 2000 *Appl. Phys. Lett.* **76** 3706
[12] Teter D M and Hemley R J 1996 *Science* **271** 53
[13] Dong J, Sankey O F, Deb S K, Wolf G and McMillan P F 2000 *Phys. Rev.* B **61** 11979
[14] Dong J, Deslippe J, Sankey O F, Soignard E and McMillan P F 2003 *Phys. Rev.* B **67** 094104
[15] Gao F, Xu R and Liu K 2005 *Phys. Rev.* B **71** 052103
[16] Ching W Y and Rulis P 2006 *Phys. Rev.* B **73** 045202
[17] Ching W Y, Mo S-D, Ouyang L, Rulis P, Tanaka I and Yoshiya M 2002 *J. Am. Ceram. Soc.* **85** 75
[18] Jansen J F and Freeman A J 1984 *Phys. Rev.* B **30** 561
[19] Hahn T 1992 *International Tables for Crystallography* 3rd revised edn, vol A (Dordrecht: Kluwer–Academic)
[20] Perdew J P and Wang Y 1992 *Phys. Rev.* B **45** 13244
[21] Perdew J P, Burke S and Ernzerhof M 1996 *Phys. Rev. Lett.* **77** 3865
[22] Blaha P, Schwarz K, Madsen G K H, Kvasnicka D and Luitz J 2001 *WIEN2k* An Augmented Plane Wave + Local Orbitals Program for Calculating Crystal Properties (Karlheinz Schwarz, Techn. Universität Wien, Austria) ISBN 3-9501031-1-2
[23] Schwarz K, Blaha P and Madsen G K H 2002 *Comput. Phys. Commun.* **147** 71
[24] Madsen G K H, Blaha P, Schwarz K, Sjöstedt E and Nordström L 2001 *Phys. Rev.* B **64** 195134
[25] Blochl P E, Jepsen O and Andersen O K 1994 *Phys. Rev.* B **49** 16223
[26] Fox P A, Hall A D and Schryer N L 1978 The PORT mathematical subroutine library *ACM Trans. Math. Softw.* **4** 104–26
[27] Ching W Y, Mo S-D and Ouyang L 2001 *Phys. Rev.* B **63** 245110
[28] Murnaghan F D 1944 *Proc. Natl Acad. Sci. USA* **30** 244
[29] Hedin L 1965 *Phys. Rev.* **139** A796
[30] Weinberg Z A and Pollak R A 1975 *Appl. Phys. Lett.* **27** 254
Karcher R, Ley L and Johnson R L 1984 *Phys. Rev.* B **30** 1896
Carson R D and Schnatterly S E 1986 *Phys. Rev.* B **33** 2432
Iqbal A, Jackson W B, Tsai C C, Allen J W and Bates C W 1987 *J. Appl. Phys.* **61** 2947
[31] Chambouleyron I and Zanatta A R 1998 *J. Appl. Phys.* **84** 1